Spectral Solar Radiation Characteristics Under Desert Conditions

Dunia Bachour[1], Daniel Perez-Astudillo[1]

[1] Qatar Environment and Energy Research Institute (QEERI), Qatar Foundation/HBKU, Doha (Qatar)

Abstract

Ground-level solar spectral measurements, which are scarce in general, are important to assess the performance of photovoltaic (PV) technologies. Indeed, PV materials have different responses with regards to the spectral distribution of solar radiation. In order to study the impact of solar spectral variations on PV, the terrestrial solar spectrum needs to be characterized and quantified. In this work, we present the analysis of solar spectral irradiance measurements recorded for a period of one year, in desertic atmospheric conditions. The spectral measurements are done on a tilted surface at an angle equal to the latitude of the studied location, and wavelength range from 350 nm to 1050 nm. The analysis covers several temporal resolutions. Moreover, the local spectral variations are characterized in terms of the variations in the average photon energy (APE) parameter as well as the useful fraction (UF) parameter specific to different PV technologies.

Keywords: Solar spectral measurements, PV performance, APE, UF, Desert conditions.

1. Introduction

The performance of PV devices is usually studied under Standard Test Conditions (STC) of specific meteorological and solar radiation parameters; these correspond to a cell temperature of 25°C, an irradiance of 1000 W/m^2 with a standard reference spectrum of a clear day at air mass 1.5 (AM1.5) (ASTM, 2003). Under real environmental conditions, the PV performance changes depending on the local variations of the specific parameter. In general, the broadband solar irradiance has the largest influence on PV module performance. However, the solar radiation spectrum can also have noticeable impacts. When compared to the reference spectrum, the actual solar spectrum at ground level varies continuously, with the changing atmospheric contents and the relative optical path of the radiation through the atmosphere. These variations in the spectral distribution of the incident solar radiation can influence the PV output under real outdoor conditions, given that different PV devices exhibit different spectral responses, with an effective spectral range specific for each (Betts, 2004). The spectral gains or losses under real operating conditions as compared to the reference conditions are quantified using a spectral factor parameter that takes into account the spectral response of the different PV technologies, and the variations of the incident solar radiation spectrum.

Several authors have studied the impact of the spectral variations on PV systems, using different module technologies at different geographical locations. Wilson and Hennies (1989) assessed the spectral variations effect on the short circuit current of GaAs and monocrystalline, polycrystalline and amorphous Si solar cells. Fabero and Chenlo (1991) studied the influence of the annual and daily variations of the spectral solar irradiance on mc-Si and a-Si devices in Spain. Nann and Emery (1992) studied the spectral effect on seven solar cells and found that the efficiencies of amorphous silicon cells differ by 10% between winter and summer months. Williams et al. in 2003 reported that the spectral impact is less pronouced for PV technologies with narrow band gaps, i.e., wide spectral response, such as CIGS or c-Si, but have a noticeable effect on materials with wide band gap, such as a-Si or CdTe. A study in Hungary (Kocsány et al., 2010) found that, in clear days, polycrystalline silicon performs better than amorphous silicon when the red and infrared bands dominate the spectrum. Virtuani and Fanni (2014) found that c-Si performs better than a-Si for a red-shifted spectrum, while a-Si outperforms c-Si for a blue shift. Alonso et al. (2014) studied the spectral effects on eight solar cell technologies and found that narrower band gaps result in higher sensitivity to spectral changes. According to Dirnberger et al. (2015), the spectral variations resulted in output changes ranging from 0.6% for small-band-gap CIGS, to 3.4% for a-Si, with c-Si (2 types) and CdTe in between, with 1.1 to 1.4%, and 2.4%, respectively. More recently, Yandt et al. (2017) studied the spectral effect on multijunction devices and reported that mismatches between junctions result in additional losses and require more detailed spectrum studies. It is thus important to study and characterize the solar spectral distribution in a specific location, for at least a period of one year, and consider the resulting variations when evaluating the outdoor performance of PV modules.

This work presents a study of the variations of the solar spectrum in a highly aerosol-loaded atmosphere, including the analysis of the local changes of the spectral distribution of the solar radiation in the range 350 nm to 1050 nm,

Selection and/or peer review under responsibility of Scientific Committee
doi:10.18086/swc.2021.37.01 Available at http://proceedings.ises.org

covering different seasons and weather conditions in a one-year period. It also includes the analysis of two parameters useful to characterize the spectral effect: the Average Photon Energy, or APE (Minemoto, 2009), commonly used to show the shift towards the red or the blue part of the spectrum, and the Useful Fraction, or UF (Gottschalg, 2003), used to account for the specific spectral response of PV devices under real local solar spectrum conditions.

2. Methodology

The solar spectral radiation was acquired using an EKO MS-700 spectroradiometer. The sensor consists of a high-quality hermetically sealed dome and diffuser that measures the spectral irradiance in the range 350 to 1050 nm, with a spectral resolution of 10 nm, wavelength accuracy of ± 0.3 nm, and a cosine error < 7%. The spectral radiometer was installed on a tilted surface at the optimal tilt of PV panels for the location under study, namely Doha, Qatar (25° N, 51° E). The solar spectral irradiance data was collected every 5 minutes from sunrise to sunset, recording 701 spectral measurements at each data acquisition, for a period of one year.

The Average Photon Energy, defined as the average energy per photon of the spectrum, is calculated according to:

$$APE = \frac{\int_0^{\lambda} G(\lambda)d\lambda}{q\int_0^{\lambda} \Phi(\lambda)d\lambda} \qquad \text{(eq. 1)}$$

Where G(λ) is the spectral irradiance, Φ is the photon spectral flux density and q is the electron charge. The integration is done over the spectral range of the spectroradiometer.

The Useful Fraction, the part of the solar spectrum which is usefully converted into electricity by the specific PV device, is calculated as follows:

$$UF = \frac{\int_0^{\lambda} G(\lambda)d\lambda}{\int_0^{\infty} \mathrm{G}(\lambda)d\lambda} \qquad \text{(eq. 2)}$$

Where G(λ), the spectral irradiance, is integrated over the spectral response of the considered PV technology at the numerator, and integrated over the whole solar spectrum at the denominator.

3. Results and discussion

As an example, the spectral irradiance collected in Doha in April 2015 is shown in Figure 1 for various times during a clear day (top graphs), and a dusty (more heavily in the morning) day (bottom graphs). On the right side, the daily profiles of the broadband solar radiation of those particular days are shown to confirm the conditions of the day.

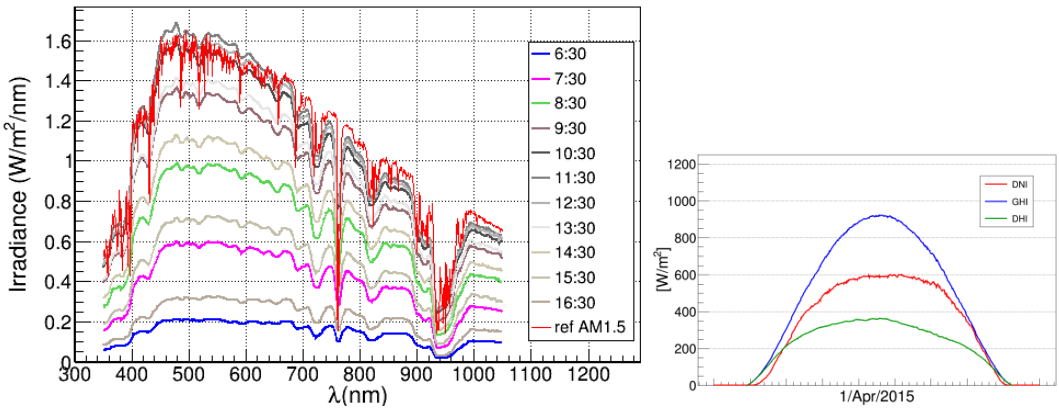

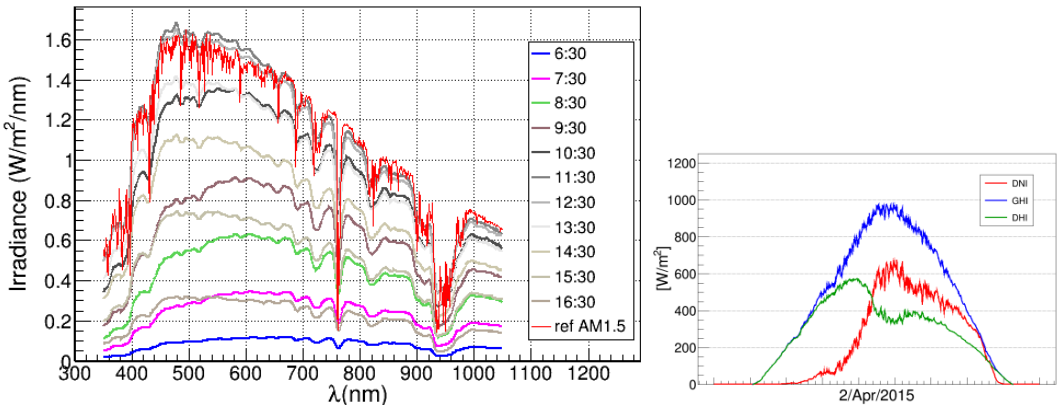

Fig. 1: Measured spectral solar radiation for various times in a clear day (top), and a dusty day (bottom) of the same month, in comparison with the ASTM AM 1.5 reference spectrum.

The absorptions of different atmospheric components at specific wavelengths are clearly seen in the spectral distribution plots. The variations within one day are due to the different paths that the solar radiation has to cross to reach the earth surface, as well as to the different atmospheric conditions encountered along this path. The path length is quantified by the Air Mass (AM) parameter, which is the ratio between the length of the path that the sun takes through the atmosphere to the shortest possible path length when the sun is directly overhead. Figure 2 shows the variations of the air mass in Doha, during one day, and during a full year period at solar noon, the solar noon being the time of the day where the sun reaches its highest apparent position in the sky, i.e. the smallest AM in each daily plot. During one day, AM decreases and increases exponentially in the morning and afternoon respectively, with the lowest value observed at solar noon. The annual variation of the AM at solar noon in Doha shows that the AM values range between 1 and 1.5 with the lowest value ~ 1 observed in June (day 172 in Figure 2, right side). The different path lengths and their different contents affect the absorption and scattering of the solar radiation and hence lead to a different solar spectral distribution in one day, and throughout the year. The influence of the atmospheric particles on the variations of the spectral radiation is obvious when we compare the spectrum plot of the clear day and dusty day in Figure 1 at a specific time (same-color line in the top and bottom plots), knowing that the change in AM is small between these two days (0.2 %). For the clear day, the irradiances are higher and the variations per wavelength are higher when compared to the dusty day during the morning hours. This is due to the strong absorption of the solar radiation by the dust particles, leading to lower variations per wavelength as the sun passes through the atmosphere, mainly in the visible wavelength range between 400 nm to 700 nm.

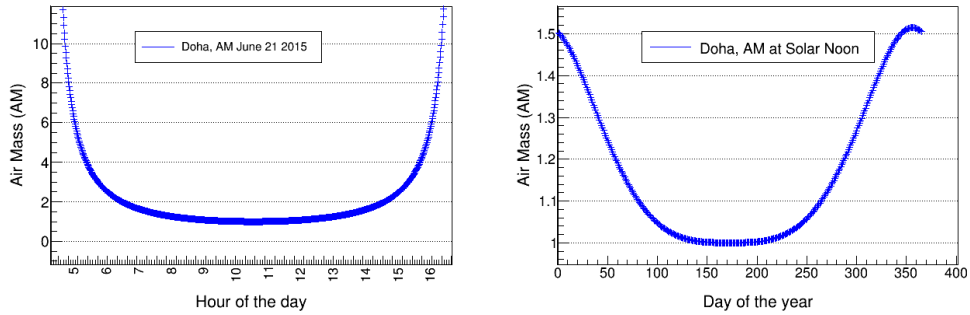

Fig. 2: Variation during one day (left), and variation through the year at solar noon (right), of air mass in Doha.

The reference spectrum shown in red in Figure 1 is the American Society for Testing and Materials (ASTM) G-173 spectrum, representing the global total solar spectral irradiance on an inclined plane of 37° tilt toward the equator and for specified atmospheric conditions, namely the 1976 U.S. Standard Atmosphere and an absolute air mass of 1.5, etc. This spectrum is used as a common reference for evaluating PV materials. The reference spectrum plotted here is adapted from the ASTM G-173-03 table published as a spreadsheet on the NREL website (NREL). It is noted that the spectra approaching the reference one in Figure 1.a and b are those measured at 11:30 hrs, the closer time of the day to the local solar noon. However, for the remaining time of the day, with the conditions being different, the measured spectral distribution deviates from the reference conditions, depending on the position of the sun and the atmospheric contents as discussed above. In order to understand better the daily variations of the spectral distribution, we calculate the average irradiance per wavelength at the same time stamp for all the days of one month, and we

determine the standard deviation relative to the average during this month. Figure 3 shows a sample of this calculation for two months, April and August, at two different time stamps, 9:00 and 11:45 am. The colored bands indicate the standard deviation bars of the averaged values, i.e. the variations of the spectral distribution during one month. For comparison, we also plot the reference spectrum AM1.5, the spectrum in blue. In April, similar spectral variations are seen in the morning (9 am) and around solar noon (11:45 am). In August, the variations are more pronounced than in April, and at solar noon they are larger than in the morning. These large variations indicate that in August the atmospheric contents are highly variable, leading to the large changes in the spectral distribution from a day to another. The closer look in Figure 4 shows bigger variations within the visible range.

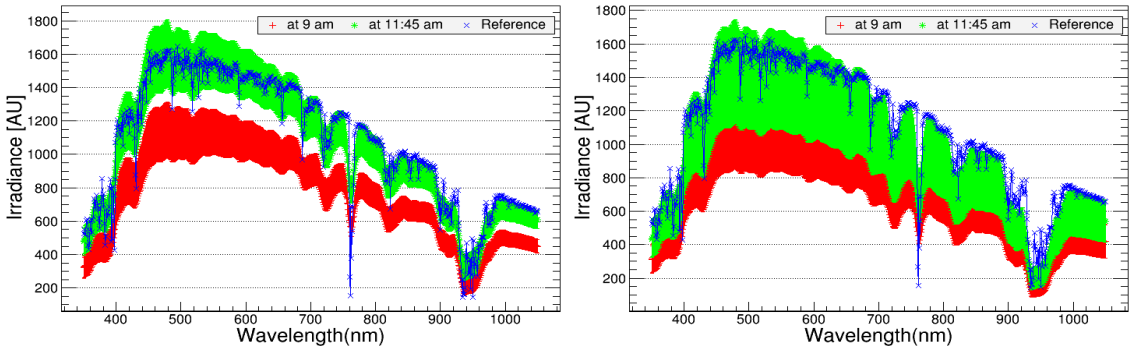

Fig. 3: Averaged spectral distribution in a month with one standard deviation bands. April (left) and August (right).

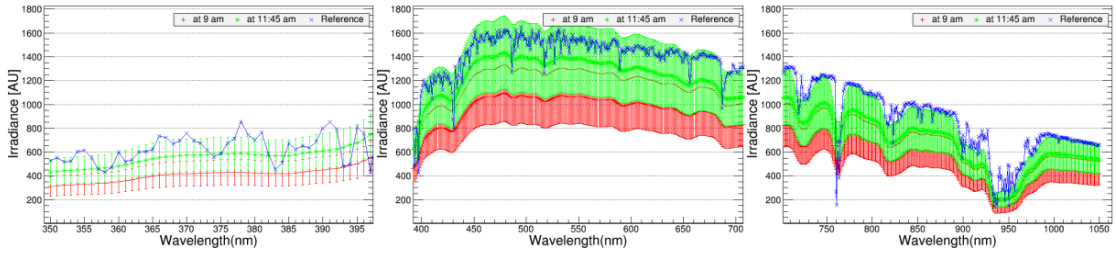

Fig. 4: Averaged spectral distribution in August with one standard deviation bands for different wavelength ranges. Ultraviolet (left), visible (middle) and near infrared (right).

As seen above, the spectral distribution of the solar radiation exhibits intra-day, daily, and seasonal variations throughout the year. Since PV cells nominal power is determined against the reference spectrum AM1.5, it is important to evaluate the spectral response of PV cells in real outdoor conditions at the location of interest, and to determine the deviations of the real measured spectra against the reference one. However, it is a cumbersome process that involves a huge amount of data when doing this analysis for each measured spectrum; for the study here, the spectrum is measured every 5 minutes, each time with 701 data points covering the range of 350 to 1050 nm. Determining one quantity, the average photon energy (APE), was found to be a suitable method that provides information about the shift of the spectrum to the blue or red wavelengths, and allows an easier way to classify the PV technologies under the real spectral conditions (Norton, 2015). The reference value APEref ~ 1.88 eV is calculated for the reference spectrum using equation 1 and considering the spectral range of the spectroradiometer (350-1050 nm). A spectrum with an APE lower than APEref is shifted towards the red wavelenghts, and higher values indicate a shift towards blue wavelengths.

In the following, we study the variations of APE in Doha, for several temporal resolutions. Figure 5 shows the frequency distribution of the 5-min APE (left) and daily APE values (right) calculated for one year, in Doha. The mean value of both distributions is equal to APEref. Considering the full year, the 5-minute values are shifted toward the blue wavelengths, and the daily values are equally distributed around the average with higher frequency for the values above the average, so that the overall spectral distribution in Doha is shifted towards the blue wavelengths.

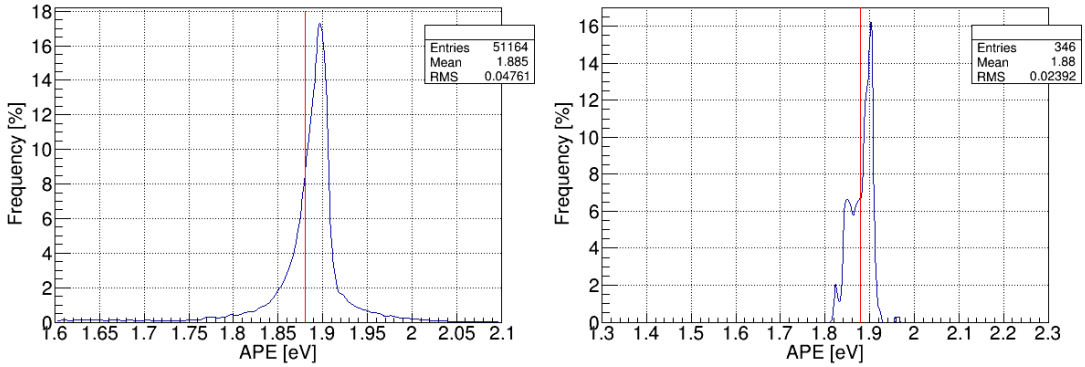

Fig. 5: Frequency distribution of APE in one year in Doha. 5-min APE (left) and daily APE (right).

Figure 6 shows the variations of the hourly APE for the two days studied in Figure 1. Comparing the clear and the dusty day, we can clearly see the low APE values in the morning hours due to the dust layer in the atmosphere, shifting the spectrum of the solar radiation to the red wavelengths (APE less than the reference APE). With the dust layer decreasing in the afternoon for the dusty day (see the daily solar radiation profile in Figure 1), APE increases to stabilise around the average, decreasing slightly around the sunset hour. To note that for this particular day in April, the sunset hour is at 17.50 pm, however the 5-min APE values used here are only provided until 17.30 pm, so the corresponding hourly APE at sunset hours (17 to 18), timestamp 17, uses only 6 APE entries, providing thus a higher APE value than expected. For the clear day. The hourly APE variations look more stable during the clear day.

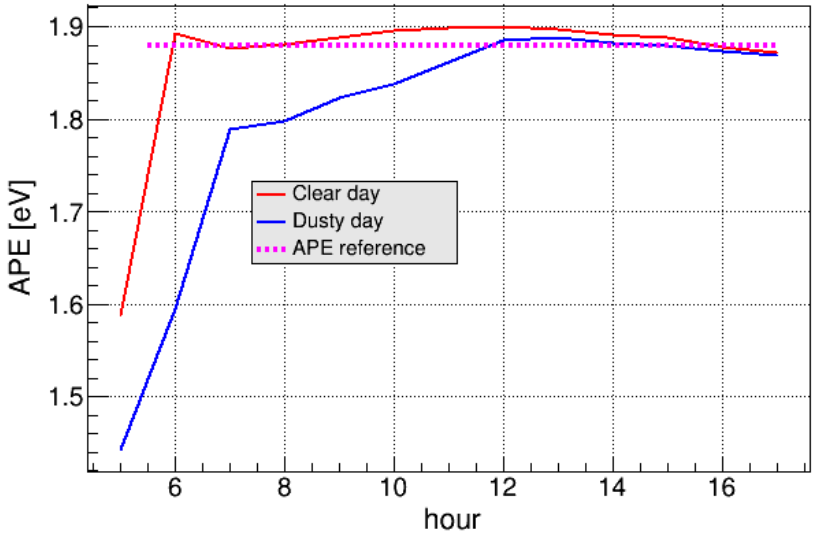

Fig. 6: Hourly APE during a clear and a dusty day.

Figure 7 shows a heatmap of the hourly APE values for one year in Doha, where the x-axis presents the hour of the day and the y-axis the hourly APE values. The color-coded scale on the right indicates the frequency distribution (in %) of APE at the corresponding hour and APE bin through the year, from purple (lowest) to red (highest); for instance, the green color in the middle means that 0.8 % of the APE values fall within the corresponding hour and APE bin. The red horizontal line is the reference APE. In general, APE values higher than the average are more frequent, with the highest frequencies seen around solar noon. More variations of APE are observed in the morning and afternoon hours due to large AM and exponential decrease/increase of AM at these hours; the asymmetry, however, reflects the more foggy early morning conditions seen in Doha. The overall spectral distribution indicates the shift to the blue wavelengths (APE higher than APEref) for all the hours of the day.

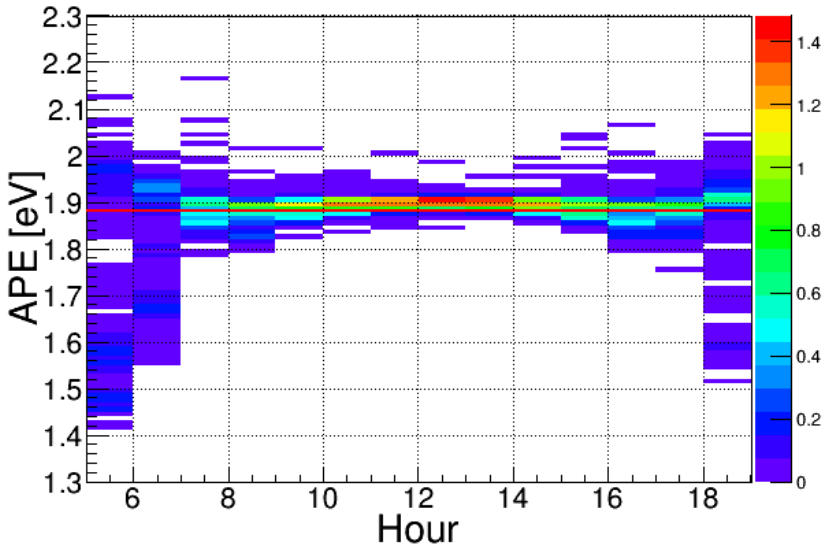

Fig. 7: 2-D histogram of hourly APE for one year in Doha. The red horizontal line indicates the reference value.

Figure 8 shows the monthly variation of APE, as compared to the reference APE value of 1.88 eV of the standard AM1.5 spectrum in the range of 350–1050 nm. High values of the monthly-averaged APE are noted in general, with values shifted towards the blue part of the spectrum for almost 8 months from March until October (October being on the edge). For the winter months, the APE is lower and indicates a shift towards the red wavelengths.

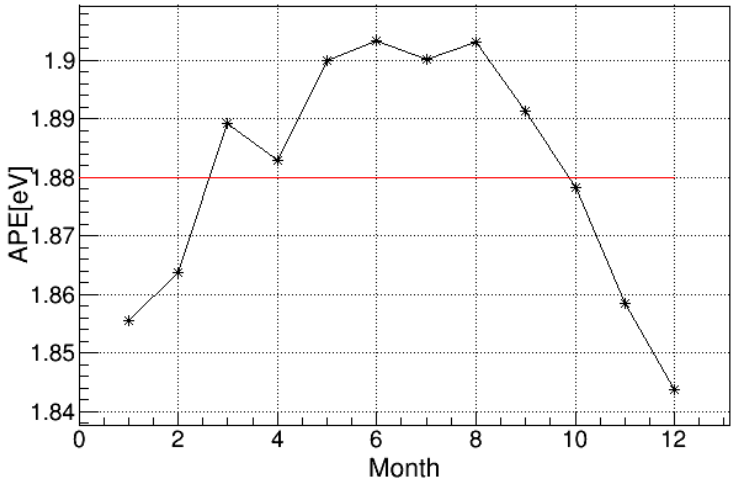

Fig. 8: Monthly variation of APE, as compared to the reference value in red.

In order to study the effect of spectral shift on a specific PV technology, the useful fraction (UF) parameter that considers the active spectral wavelength band of PV materials is used. In this contribution, we consider two cases with useful spectral range from 350-800 nm and 350-900 nm. The two wavelengths 800 nm and 900 nm correspond to the upper wavelength limit of the spectral response of a-Si and CdTe, respectively. Due to the range of the sensor used here, we use 350 nm as the lower limit of the useful spectral range. The UF reference is calculated from the reference spectrum AM1.5 in the measured spectral band (350-1050 nm); UF is 0.76 for the spectral range 350-800 nm and 0.88 for the 350-900 nm spectral range. Figure 9 shows the frequency distribution of UF for one year in Doha for the two spectral ranges considered here. The red line is the UF reference value. Figure 10 (left side) shows the monthly-averaged UF, with bars at each monthly value indicating the standard deviation of UF during the corresponding month. The dashed horizontal lines are the reference values.

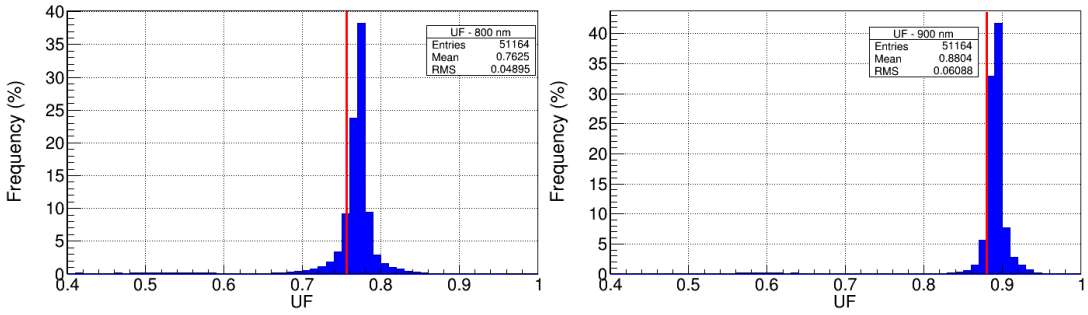

Fig. 9: Frequency distribution of useful fraction (UF), up to 800 nm (left) and up to 900 nm (right). The red vertical line is the reference UF.

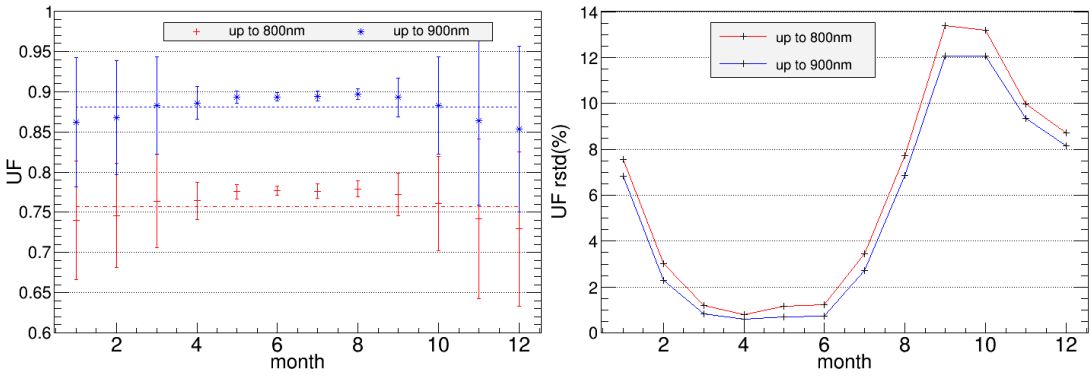

Fig. 10: Monthly variations of useful fraction (UF) for two PV technologies. Averaged values with one-standard deviation bars (left), standard deviation in percentage (right).

The frequency distribution of UF values in Figure 9 shows that more UF values are above the reference spectrum value for the two ranges studied here. Higher UF values are calculated for the higher spectral range as expected. In figure 10 (left), the monthly variations shows that the high UF values occurs mostly at summer months, from April to October, with low variations in UF (smaller standard deviation bars), while the winter months show lower UF values but with larger variations. UF variations during each one-month period are higher for the smallest spectral band for all the months as seen on the right side of Figure 10, showing the relative standard deviations of UF.

4. Conclusion

Solar PV technologies are rated under the specific conditions of the reference spectrum AM1.5. However, due to intra-day and annual variations of the path lengths of the solar radiation, as well as the changes in the atmospheric contents, the real spectrum exhibits significant variations. It is thus crucial to characterize the spectral distribution in locations of interest for PV technologies, in order to determine the effect of these variations on the performance of PV cells in real outdoor conditions.

In this work, we presented the analysis of solar spectral irradiance measurements recorded for a period of one year, in desertic atmospheric conditions. The spectral measurements are done on a tilted surface at the latitude of the studied location, and for a spectral range from 350 nm to 1050 nm. The analysis covered several temporal resolutions, and the local spectral variations were characterized in terms of the variations of the two parameters, the average photon energy (APE) and the useful fraction (UF, which depends on the spectral range of the different PV technologies). From this analysis, we found that the overall spectral solar radiation in Doha is shifted towards the blue wavelengths for the ‘summer’ months and towards the red wavelengths during the ‘winter’ months. However and independently from the season, these averaged conditions change when local conditions such as dusty conditions occur, and shift the spectrum towards the red wavelengths. When studying the spectrum in the wavelength ranges that are similar to the response of some technologies, it was found that PV technologies with smaller wavelength range are more affected by the local spectral variations. This emphsasises the importance of including the characterization of the solar spectral irradiance measurements in the evaluation of PV modules performance and yield in real operating conditions.

5. References

Alonso-Abella, M., Chenlo, F., Nofuentes, G., Torres-Ramírez, M., 2014. Analysis of spectral effects on the energy yield of different PV (photovoltaic) technologies: The case of four specific sites. Energy 67, 435-443. DOI:10.1016/j.energy.2014.01.024

ASTM, 2003. Standard tables for reference solar spectral irradiance at air mass 1.5: Direct normal and hemispherical for a 37° tilted surface. Standard G173-03, American Society for Testing and Materials, West Conshohocken, PA.

Betts, T. R., 2004. Investigation of photovoltaic device operation under varying spectral conditions. Doctoral dissertation, Loughborough University.

Dirnberger, D., Blackburn, G., Müller, B., Reise, C., 2015. On the impact of solar spectral irradiance on the yield of different PV technologies. Solar Energy Materials and Solar Cells 132, 431-442. DOI:10.1016/j.solmat.2014.09.034

Fabero, F., Chenlo, F., 1991. Variance in the solar spectrum with the position of the receiver surface during the day for PV applications. 22nd IEEE Photovoltaics Specialists Conference, 812–817. DOI: 10.1109/PVSC.1991.169321

Gottschalg, R., Betts, T.R., Infield, D.G., Keamey, M.J., 2003. Experimental study of variations of the solar spectrum of relevance to thin film solar cells. Solar Energy Materials & Solar Cells 79, 527–537. DOI:10.1016/S0927-0248(03)00106-5

Kocsány, I., Seres, I., Farkas, I., Weihs, P., 2010. Solar Energy Potential and its Spectral Distribution under Different Climate Conditions. Proceedings of ISES Eurosun 2010 Conference, Austria. DOI:10.18086/eurosun.2010.13.03

Minemoto, T., Nakada, Y., Takahashi, H., Takakura, H., 2009. Uniqueness verification of solar spectrum index of average photon energy for evaluating outdoor performance of photovoltaic modules. Solar Energy 83(8), 1294-1299. DOI:10.1016/j.solener.2009.03.004

Nann, S., Emery, K., 1992. Spectral effects on PV-device rating. Solar Energy Materials and Solar Cells 27 (3), 189-216. DOI:10.1016/0927-0248(92)90083-2

Norton, M., Gracia Amillo, A.M., Galleano, R., 2015. Comparison of solar spectral irradiance measurements using the average photon energy parameter. Solar Energy 120, 337-344. DOI:10.1016/j.solener.2015.06.023

NREL reference Air Mass 1.5 Spectra. https://www.nrel.gov/grid/solar-resource/spectra-am1.5.html. Last accessed October 2021.

Virtuani, A., Fanni, L., 2014. Seasonal power fluctuations of amorphous silicon thin-film solar modules: distinguishing between different contributions. Progress in Photovoltaics: Research and Applications 22 (2), 208-217. DOI:10.1002/pip.2257

Williams, S.R., Betts, T.R., Vorasayan, P., Gottschalg, R., Infield, D.G., 2005. Actual PV module performance including spectral losses in the UK. 31st IEEE Photovoltaic Specialists Conference, 1607-1610. DOI:10.1109/PVSC.2005.1488452

Wilson, H. R., Hennies, M., 1989. Energetic relevance of solar spectral variation on solar cell short circuit current. Solar Energy 42, 273–279. DOI:10.1016/0038-092X(89)90018-2

Yandt, M., Hinzer, K., Schriemer, H., 2017. Efficient Multijunction Solar Cell Design for Maximum Annual Energy Yield by Representative Spectrum Selection. IEEE Journal of Photovoltaics 7(2), 695-701. DOI: 10.1109/JPHOTOV.2016.2638040